Polymer 51 (2010) 4077–4086

Contents lists available at ScienceDirect

Polymer

journal homepage: www.elsevier.com/locate/polymer

Synthesis and characterization of poly (ethylene oxide) containing copolyimides for hydrogen purification

Hangzheng Chen, Youchang Xiao, Tai-Shung Chung*

Department of Chemical & Biomolecular Engineering, National University of Singapore, 10 Kent Ridge Crescent, Singapore 119260

ARTICLE INFO

Article history:
Received 1 February 2010
Received in revised form
3 June 2010
Accepted 24 June 2010
Available online 7 July 2010

Keywords:
Poly(ethylene oxide) PEO
PEO containing copolyimide(PEO-PI)
Hydrogen purification

ABSTRACT

Reverse selective membranes comprising poly(ethylene oxide) (PEO) containing copolyimides (PEO-PI) with variations of acid dianhydrides and diamines have been synthesized for hydrogen purification. The reverse selectivity of the membranes decimate the energy required for hydrogen recompression process. Factors including PEO content, PEO molecular weight, and fractional free volume (FFV) that would affect the gas transport performance have been investigated and elucidated in terms of degree of crystallinity, phase separation in the PEO domain as well as inter-penetration between the hard and soft segments. In mixed gas tests of CO_2 and H_2 mixtures, a highly condensable CO_2 out compete H_2 for the sorption sites in hard segment and diminishes H_2 permeability. Thus the CO_2/H_2 selectivity in the mixed gas tests is much higher than that in pure gas tests. Mixed gas permeation tests at 35 °C and 2atm show that the best reverse selective membranes have a CO_2 permeability of 179.3 Barrers and a CO_2/H_2 permselectivity of 22.7. The physical properties of PEO-PIs have also been characterized by FTIR, DSC, GPC, WAXS, AFM and tensile strain tests.

1. Introduction

Global warming resulting from the emission of greenhouse gases is a worldwide environmental concern. Hence one of the major challenges faced by researchers around the world is to develop advanced technologies to reduce the emission of greenhouse gases. Since much of the world's energy consumption is based on crude oil, it releases a large amount of greenhouse gases, while the demand for crude oil is continuously increasing, the search for an affordable and clean alternative energy is of paramount interest to the global community [1,2]. Hydrogen is a potential solution because it is a clean energy and an important feedstock in the petrochemical industry.

Hydrogen does not exist alone in nature, but it can be produced from a wide variety of energy sources like natural gas, coal and biomass. The steam reforming of natural gas is the current dominant industrial process for hydrogen production [3]; about 80% of the world's hydrogen supply are synthesized from this process. However, the steam reforming produces many by-products like CO_2, CH_4, H_2O and CO, which have to be removed from the production stream before the efficient utilization of the produced hydrogen [4]. Pressure swing adsorption (PSA) and cryogenic distillation are the most conventional methods used for the purification of hydrogen [5,6]. Although these two techniques can produce high purity hydrogen, they have drawbacks of consuming a large amount of energy and occupying a big footprint. Membrane is an emerging technology that displays attractive advantages over such conventional methods such as (1) high energy efficiency, (2) cost effectiveness with smaller footprint, (3) simplicity in operation, (4) compactness and portability, and (5) environmental friendliness [7,8]. Various materials such as zeolites, metals and polymers have been reported as membrane materials for hydrogen purification applications. However, polymers have advantages over others because of easy process and reasonably low costs.

It is well known that the gas transport through polymeric membranes is dictated by the solution diffusion mechanism and the permeability of the membrane is a product of diffusivity and solubility. Resulting from the counter balance between high hydrogen diffusivity coupled with high CO_2 solubility, it is challenging to separate hydrogen from CO_2. Since the solubility selectivity in traditional glassy polymers varies slightly with most gas species, the selectivity of glassy polymeric membrane for gas separation is almost dominated by diffusivity selectivity. Since H_2 possesses a smaller kinetic diameter as compared to CO_2 and hence diffuses more easily, glassy polymeric membranes tend to be classified as H_2 selective membranes [9-11]. However, there is a trade-

* Corresponding author. Tel.: +65 6874 6645; fax: +65 6779 1936.
E-mail address: chencts@nus.edu.sg (T.-S. Chung).

0032-3861/$ – see front matter © 2010 Elsevier Ltd. All rights reserved.
doi:10.1016/j.polymer.2010.06.046

off between H_2 permeability and H_2/CO_2 selectivity for glassy polymeric membranes [12]. Chung's group has reported a polyimide crosslinking methodology using various types of diamines to surpass the aforementioned trade-off by increasing diffusivity selectivity [13–16]. Hydrogen selective membranes have good chemical and thermal stability and excellent mechanical property, but the choice of this type of membranes is largely dependent on the operating conditions and industrial applications.

Perhaps, Kawakami et al. were the pioneers discovering that PEG and other polymer blends had good separation performance for CO_2/light gas mixtures [17]. Since the P_{CO_2}/P_{N_2} ratio increased with an increase in PEG content, while P_{O_2}/P_{N_2} remained the same, they reported there was an enhanced interaction between ethylene glycol (EG) and CO_2 in the PEG blend membrane. However, it was found that the membrane mechanical strength was reduced and became too weak for gas separation when the PEG content reached more than 60 wt%. Okamoto et al. synthesized the first PEO-PI membranes for CO_2/N_2 separation [18–20] and reported a CO_2 gas permeability of 140 Barrers and a CO_2/N_2 selectivity of 70. The high CO_2/N_2 selectivity was attributed to high solubility selectivity due to strong interactions between CO_2 and the PEO phase, as ethylene oxide was identified as the best chemical group interacting favorably with CO_2. Since then the interaction between CO_2 and EO has been discussed and used for the development of CO_2 selective membranes in many publications [21–26]. Zhao et al. demonstrated that PEG bis (amine) can be used as a crosslinking agent to modify a Matrimid membrane and switch the membrane selectivity from being H_2 selective to CO_2 selective after the chemical modification [27]. Other researchers like Lin et al. invented a highly branched, cross-linked PEO membrane for CO_2/H_2 separation [28]. Again, the high CO_2/H_2 selectivity was due to favorable interactions between the EO unit and CO_2 gas. As a result, the penetrant with a higher condensability (CO_2) will end up as the main product in the permeate side and make the membrane to be CO_2 selective. However, the characteristics of weak mechanical properties and easy crystallization are the main drawbacks of PEO-based membranes. Recently, Shao and Chung fabricated a cross-linked PEO/silica reverse selective membrane for hydrogen purification [29]. This cross-linked organic-inorganic hybrid membrane had improved mechanical strengths and reduced crystallization in comparison with a pure PEO membrane. No crystallization was reported at 75% silica loading in their membranes, which is especially desirable in gas separation as crystals reduce the overall gas permeability. Since the Robeson upper bound of CO_2 selective membranes display a positive slope when plotting selectivity versus permeability, it implies that such membranes can achieve high CO_2 permeability whilst yielding impressive CO_2/H_2 selectivity [28].

Although pure PEO polymers have demonstrated very good CO_2 removal capability, they are not robust enough for real industrial applications due to their weak mechanical properties, easy crystallization, and low thermal stability. However, their potential energy saving and high CO_2 removal efficiency have inspired us to investigate PEO-PI membranes for the H_2 purification process. The combination of PEO and PI via proper molecular engineering may take advantages of both glassy and rubbery polymers for CO_2 and H_2 separation and the resultant membranes may have balanced thermal and chemical stability because of directly chemical bonding between the PEO units and the hard polyimide segments.

2. Experimental section

2.1. Materials

3,3′,4,4′ benzophenonetetracarboxylic dianhydride (BTDA) from Lancaster, 4,4′-(hexafluoroisopropylidene) diphthalic anhydride (6FDA), pyromellitic dianhydride (PMDA), 1,3-phenylenediamine (mPD), 2,3,5,6-tetramethyl-*p*-phenylenediamine (Durene), 4,4′-oxydianiline (ODA) and polyoxyethylene bis(amine) with molecular weights of 1900, 10 000 and 20 000 g/mol were obtained from Sigma–Aldrich Co. Fig. 1 shows their chemical structures. The polyoxyethylene bis(amine) was used without further purification, while the rest of monomers were purified by vacuum sublimation except 2,3,5,6-tetramethyl-*p*-phenylenediamine (Durene) which was purified by re-crystallization in methanol. *N*-methyl-2-pyrrolidinone (NMP) from Merck was used as solvent after purified by vacuum distillation. The purities of H_2 and CO_2 were 99.99%.

2.2. Preparation of PEO containing copolyimide dense films

All the copolymers studied in this paper were synthesized in our laboratory, the procedure of the dense film preparation is as follows: The polyethylene bis(amine) and the comonomer diamine

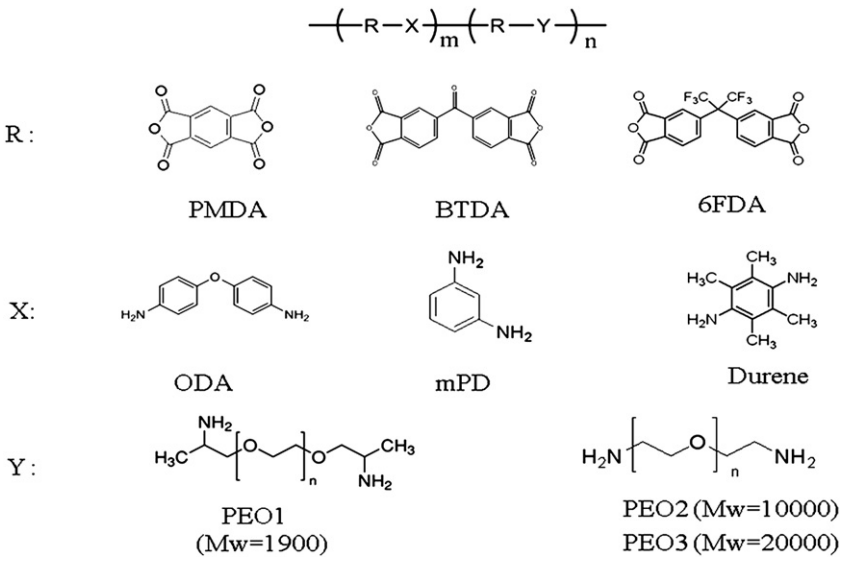

Fig. 1. Chemical structures of monomers used in this study.

were dissolved in NMP under nitrogen environment at room temperature. A stoichiometric amount of dianhydride was slowly added into a magnetically stirred flask. After all the solids were dissolved, the solution was stirred overnight. The resultant 10 wt% copoly(amic acid) solution was filtered using a 1.0 μm PTFE membrane before casting onto a Teflon petri-dish. The solution was dried under vacuum at 80 °C for 12 h that allowed slow solvent evaporation. The temperature was increased by 12 °C at 20 min interval until it reached 200 °C. The membranes were thermally imidized at 200 °C for 24 h under vacuum and then it was cooled down naturally. The thicknesses of the films were in the range of 50–150 μm. Throughout this article, the number in the parenthesis is referred to the weight percentage of polyether diamine to the total weight of the copolymer.

2.3. Characterizations

The chemical structures of the PEO containing copolyimides were analyzed using a Bio-Rad FTIR FTS 135 over the range of 700–4000 cm^{-1} in the attenuated total reflectance (ATR) mode. The number of scans for each sample was 16. The glass transition temperature (T_g) and melting temperature (T_m) were determined using differential scanning calorimetry (DSC) via a DSC 822^e (Mettler Toledo) with a heating or cooling rate of 10 °C/min. To align with the testing temperature of gas permeation tests, crystallinity of the membranes at 35 °C was measured. The samples were hold at 35 °C for 5 min followed by a steady increase in temperature. The crystallinity was calculated from the onset enthalpy at the melting temperature. The presence of the PEO crystals at 35 °C was confirmed by using a Wide-angle X-ray diffraction, Bruker, D8 series, GADDS (general area detector diffraction system). A Cu X-ray source was used and the scanning angle was from 2 to 65°. The densities of dense membrane films were determined using a Mettler Toledo balance and a density kit according to the Archimedean principle with the aid of the following equation.

$$\rho = \frac{W_{air}}{W_{air} - W_{liq}}\rho_0 \tag{1}$$

where $\rho$is the density of the film, ρ_0 is the density of the auxiliary liquid which isooctane was used because PEO was reported to be insoluble in isooctane [30]. W_{air} and W_{liq} are the weights of the film in the air and auxiliary liquid, respectively.

The molecular weights and molecular weight distributions of the block copolymers were determined using gel permeation chromatography (GPC). The Waters GPC system consisted of a Water 1515 isocratic HPLC pump, a Waters 717 plus auto sampler and a Waters 2414 refractive index detector. The system was calibrated with polystyrene standards and using HPLC grade DMF as the mobile phase. The concentration of the sample prepared was 1 mg/ml, the flow rate of the mobile phase was set at 1 ml/min and the injection volume of each sample was 100 μL.

The mechanical properties (i.e. extension at break, tensile strength and Young's modulus) of the flat sheet membranes were measured using an Instron 5542 tensile testing instrument at room temperature. The samples were prepared with 5 mm in width and the initial gauge length of 20 mm. Each sample was clamped at the both ends and the testing speed was 10 mm/min. The mean value of at least three samples was reported for each membrane.

2.4. Measurements of gas transport properties

All the membranes were undergone pure gas permeation tests and mixed gas permeation tests. The pure gas permeability was determined by a constant volume and variable pressure method. Detailed experimental design and procedures have been reported elsewhere [31]. The testing temperature and pressure were 35 °C and 2atm, respectively. The rate of downstream pressure (dp/dt) increase at a steady state was used to calculate the gas permeability using equation (2).

$$P = \frac{273 \times 10^{10}}{760}\frac{VL}{AT(p_2 \times 76/14.7)}(dp/dt) \tag{2}$$

where P is the permeability of a membrane in Barrer (1 Barrer $= 1 \times 10^{-10}$ cm^3(STP)cm/(cm^2 s cm Hg), V is the volume of the downstream chamber (cm^3), L refers to the thickness of the membrane (cm), A is the effective area of the membrane (cm^2), T is the operating temperature (K), and the pressure of the feed gas in the upstream is given by p_2 (psia). The ideal permselectivity of a membrane for each gas pair was evaluated using equation (3).

$$\alpha^*_{A/B} = P_A/P_B = (S_A/S_B) \times (D_A/D_B) \tag{3}$$

where S and D are the solubility coefficient and diffusion coefficient of the gas, respectively; S_A/S_B and D_A/D_B are the solubility selectivity and diffusivity selectivity of the gas pair, respectively. The gas equilibrium isotherm for CO_2 was measured at 35 °C using a Cahn D200 microbalance sorption cell. Prior to test, the microbalance was calibrated using the testing gas at various pressures, the weight gained was plotted as a function of pressure. The system was evacuated for at least 24 h before loading the sample (50–100 mg) into the sample pan. The testing gas was fed into the system at a desired pressure and the gas was absorbed by the polymer matrix until it reached equilibrium. The weight gain was recorded and the same steps were repeated to test the next pressure, the system was not evacuated until the end of the test for a specific gas. The sample pan was tared to zero under vacuum at each time when starting a new sample or a new gas species. The sorption coefficient was calculated by considering the buoyancy force of the polymer in the specific gas. The solubility of the membrane for a specific gas can be calculated using equation (4) [32,33].

$$S = C/P \tag{4}$$

where C is the total absorbed gas concentration in the membrane (cm^3(STP) cm^{-3}), which is measured by microbalance sorption cell. P is the testing pressure (atm). The diffusion coefficient can be obtained after the determination of permeability and solubility coefficients of the membrane as follows:

$$D = P/S \tag{5}$$

The mixed gas permeation was measured as well, the detailed experimental setup and procedures have been reported elsewhere [34]. A binary gas mixture of 50/50 CO_2 and H_2 was used and all samples were tested at 35 °C under different feed pressures. The permeate gas was injected into a GC for analyzing when the pressure of the downstream was built up more than 50 Torr. The permeability was calculated with the consideration of non-ideal gas behavior, described by Wang et al. [35]. The permeability of each gas was obtained using equations (6) and (7):

$$P_{CO_2} = \frac{273 \times 10^{10}}{760}\frac{y_{CO_2}VL}{AT(76/14.7)(x_{CO_2}p_2)}(dp_1/dt) \tag{6}$$

$$P_{H_2} = \frac{273 \times 10^{10}}{760}\frac{(1-y_{CO_2})VL}{AT(76/14.7)(1-x_{CO_2})p_2}(dp_1/dt) \tag{7}$$

where P_{CO_2} and P_{H_2} are the permeability of CO_2 and H_2, respectively, p_2 is the upstream feed gas pressure (psia), p_1 is the downstream

permeate gas pressure (psia), x_{CO_2} is the gas CO_2 molar fraction in the feed gas and y_{CO_2} is the gas CO_2 molar fraction in the permeate, V is the volume of the downstream chamber (cm_3), L is the film thickness (cm). The selectivity of mixed gas is defined by the ratio of mole fraction ratios of the two components (CO_2 and H_2) in the downstream (y) to the upstream (x) as follows:

$$\alpha_{CO_2/H_2} = \frac{y_{CO_2}/y_{H_2}}{x_{CO_2}/x_{H_2}} \quad (8)$$

In the case of negligible downstream pressure, the selectivity ($\alpha_{A/B}$) is equal to the ideal selectivity ($\alpha^*_{A/B}$) that measured the intrinsic selectivity of membrane material. Therefore, the selectivity of gas CO_2 and gas H_2 is thus computed by equation (9), which is equivalent to the ratio of their permeabilities measured at the partial pressure:

$$\alpha_{CO_2/H_2} = P_{CO_2}/P_{H_2} \quad (9)$$

3. Results and discussion

3.1. Characterization results

The molecular weight and molecular weight distribution of the copolymers are determined using GPC. In this study, due to the insolubility of PMDA and BTDA based copolyimides after thermal treatment, the precipitate of their poly (amic acid) was tested. The solution of poly (amic acid) was precipitated in isopropyl alcohol (IPA) and dried in the oven at 70 °C under vacuum for 8 h to remove all monomers and solvent residues in the solid. The dried poly (amic acid) was then dissolved in DMF with a concentration of 1 mg/ml for GPC testing. The results of number-average molar mass M_n, weight-average molar mass M_w and polydispersity M_w/M_n from GPC test are shown in Table 1. As can be seen, the synthesized copolymers have their molecular weights greater than 20,000 Da.

The block copolymers synthesized in this study were monitored using ATR-FTIR and their spectra are shown in Fig. 2. All the block copolymer films exhibit a characteristic peak at 1717 cm^{-1} which is attributed to the asymmetric stretch of C=O in imide groups. The common peaks appearing at the wave number of 2880 cm^{-1} are from the PEO groups. The intensity of this peak increases with increasing PEO weight percentage in the PMDA-ODA-PEO1 block copolymers. The FTIR spectra show that all the synthesized polymers are PEO containing copolyimides.

Fig. 3 shows DSC curves of the PEO containing copolyimides. The glass transition temperature of PEO is clearly shown in the range of −70 °C to −30 °C for PEO1 based copolymers. However, *Tg* of PEO is not very obvious for copolymers synthesized from higher molecular weights of PEO2 and PEO3. This may be owing to the relatively low molar ratio of aliphatic diamine when a high molecular weight of PEO is used. The peak in the range of 20 °C–50 °C is attributed to

Table 1
Molecular weights and molecular weight distributions of copolymers.

Polymer Name	M_n	M_w	M_w/M_n
PMDA-ODA-PEO1(20%)	27 696	43 323	1.56
PMDA-ODA-PEO1(40%)	32 125	46 656	1.45
PMDA-ODA-PEO1(60%)	19 857	25 930	1.31
PMDA-ODA-PEO2(60%)	68 543	85 696	1.25
PMDA-ODA-PEO3(60%)	48 289	78 374	1.62
BTDA-ODA-PEO1(60%)	85 769	11 5877	1.35
6FDA-ODA-PEO1(60%)	46 526	65 235	1.40

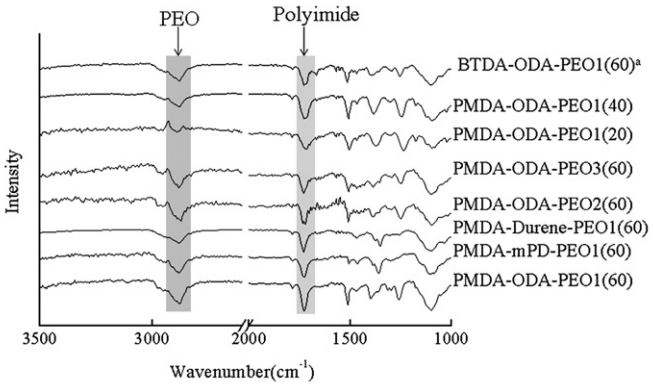

[a]The number in the parenthesis is referred to the weight percentage of PEO to the total weight of the copolymer

Fig. 2. FTIR spectra of PEO containing copolyimides.

the melting of PEO crystals. However, no endothermic peak can be found for the copolymers if the PEO content is below 60%. This implies a complete suppression of PEO crystallization by the existence of polyimide hard segments. The hard segment is the continuous phase when PEO content is low; the crystallization prone soft PEO phase is dispersed around the continuous phase. The existence of polyimide lowers the chain packing efficiency of the soft PEO phase; hence, eliminate the crystallization in PEO-PI with low PEO content. When the PEO content exceeds 60%, the soft segments form a continuous phase which promotes crystallization in the membrane. This observation is consistent with the work by Maya et al., whereby copolyimides with PEO content from 30 to 56% were amorphous but exhibited crystallinity at PEO content greater than 60% [36].

In this study, *Tg* of the hard segment is not detectable from the DSC analysis, this could be attributed to the randomization of the polymer chain formation. The hard blocks could not form a long chain due to the randomization even though the aromatic diamine has a much higher molar ratio than the aliphatic one. Table 2 shows that the degree of crystallinity varies with PEO molecular weight, indicating a general trend that the degree of crystallinity experiences a positive correlation with PEO molecular weight. As a result, the PMDA-ODA-PEO3(60) copolymer has the highest crystallinity of 37.2%. This may arise from strong chain folding characteristics in this high molecular weight PEO.

Table 2 summarizes the crystallinity level of membranes made from different moieties and percentages of PEO. The percentage of crystallinity is calculated based on the heat of fusion during melting of the PEO phase using equation 10:

$$\text{Crystallinity}(\%) = \Delta H_f / \left(\chi_p \times \Delta H_f^0\right) \times 100\% \quad (10)$$

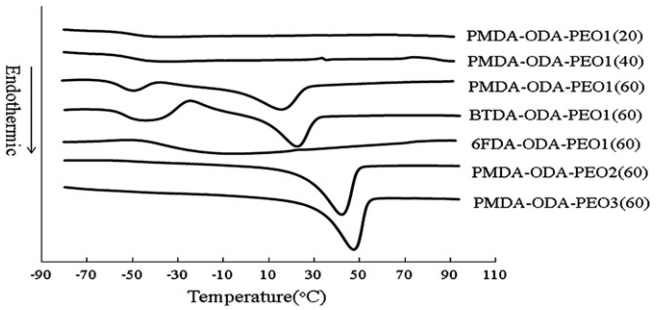

Fig. 3. DSC curves of PEO containing copolyimides.

Table 2
Density, crystallinity and mechanical properties results of copolymers.

Polymer Name	Density (g/cm3)	Crystallinity[a] (%)	Young's Modulus (GPa)	Elongation at break (%)	Tensile strength (GPa)
PMDA-ODA-PEO1(20)	1.374	ND/ND[b]	1.40	145	1.63
PMDA-ODA-PEO1(40)	1.313	ND/ND	0.60	420	0.67
PMDA-ODA-PEO1(60)	1.244	23.3/ND	0.07	535	0.10
PMDA-ODA-PEO2(60)	1.245	34.7/4.8	0.22	536	0.27
PMDA-ODA-PEO3(60)	1.231	37.2/10.5	0.24	482	0.30
BTDA-ODA-PEO1(60)	1.250	26.5/ND	0.03	248	0.06
6FDA-ODA-PEO1(60)	1.263	ND/ND	0.02	ND	ND

[a] The crystallinity is displayed at room temperature and at 35°C, respectively.
[b] ND means not detected.

where ΔH_f is the apparent heat of fusion per gram of the membrane material, ΔH_f^0 is the heat of fusion per gram of the perfect PEO crystal with a value of 188.9 J/g [37] and χ_p is the weight percentage of PEO in the block copolymer.

As our gas permeation test was done at 35 °C, the remaining crystallinity at this temperature has also been determined. At this temperature, the crystallinity is reduced drastically. There is no existence of crystals in the membranes synthesized from a low PEO molecular weight due to the melting temperature of this PEO is lower than 35 °C. However, copolymers with PEO2 and PEO3 still contain a small amount of crystallinity. Wide-angle X-ray diffraction tests were specifically carried out at 35 °C to confirm the presence of PEO crystallinity at this temperature. The spectra are showing in Fig. 4.

The PMDA-ODA-PEO1(60) membrane has no PEO crystallinity at 35 °C as the low molecular weight PEO melts at around 25 °C. The spectrum of this membrane displays similar characteristic peaks to a pure PMDA-ODA film because the PMDA-ODA polyimide itself is a semi-crystalline material. The membrane synthesized from a high molecular weight of PEO3 shows two very sharp peaks at 2θ equals to 19.2° and 23.2°, which correspond to typical PEO crystalline peaks. [36] This is consistent with the observation in the DSC test, where PEO crystallinity in PMDA-ODA-PEO3(60) still exists at 35 °C. However, no PEO crystal peaks are found in PMDA-ODA-PEO2(60). This could be attributed to the amount of PEO crystals in this membrane is too little to be detected at this temperature.

The mechanical property test results shown in Table 2 reveal that the Young's modulus is significantly affected by the PEO content in the membranes. Their values decrease as the PEO content increases; however, the Young's modulus decreases drastically when the PEO content is more than 40%. Thus, it may be concluded that the soft segment may form a continuous phase at the PEO content greater than 40%. On the other hand, these values apparently remain almost invariant with different dianhydride and diamine moieties. This implies that the membrane mechanical strength is mainly determined by the PEO weight percentage in the membrane. Since pure PEO membranes have a Young's modulus of about 0.12 GPa, the PEO containing copolyimides possess better mechanical strengths if the PEO content is less than 40 wt%.

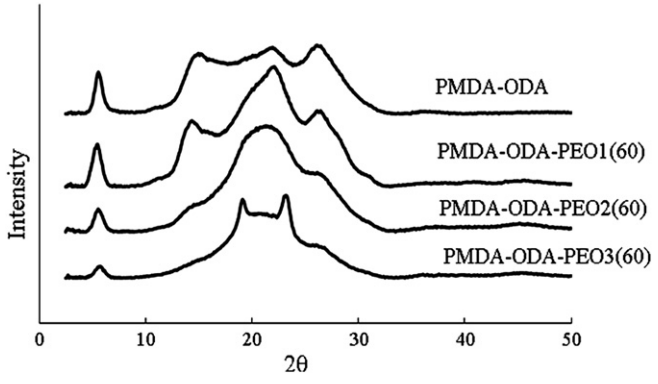

Fig. 4. WAXS spectra of PEO containing copolyimides.

3.2. Gas permeation and separation properties

3.2.1. Effect of PEO content

Sorption and pure gas permeation tests were conducted to study the gas transport properties of PEO containing copolyimides and Table 3 summarizes the results. The membranes listed in this table can be categorized into three groups for in-depth discussion of various molecular designs of PEO-PI membranes on gas transport properties.

In the copolymer of PMDA-ODA-PEO1 with different PEO weight percentages, the permeability increases with increasing PEO content. The increase in permeability can be attributed to the increase in diffusivity coefficient as PEO in the soft segment has higher polymer chain flexibility and mobility than the polyimide segment. This trend is even more pronounced when the PEO content is more than 40%, as the diffusivity coefficient increases drastically, thus increasing the CO_2 permeability.

Fig. 5 illustrates the effects of low molecular weight PEO content on the permeability, diffusivity and solubility coefficient of PMDA-ODA-PEO1 copolymers.

As can be seen, the solubility coefficient decreases with increasing PEO content. This could be attributed to the decline of the solubility contributed from the hard segment. The solubility of the hard segment (4.5×10^{-2} $cm^3(STP)cm^{-3}cmHg^{-1}$) [38] is much higher than pure PEO (1.3×10^{-2} $cm^3(STP)cm^{-3}cmHg^{-1}$) [18] as shown in Fig. 5. The portion of hard segment exists in copolymer decreases with increasing PEO content, hence the solubility coefficient decreases. At PEO content of 20%, the solubility in the hard segment is dominant. As PEO content increases, the sorption sites in the hard segment decrease and the sorption curves display a characteristic of rubbery material as shown in Fig. 6.

Table 3
Pure gas permeability, solubility and diffusivity coefficient.

Polymer Name	Permeability (Barrer)		S_{CO_2}[a]	D_{CO_2}[a]	Selectivity
	H_2	CO_2			CO_2/H_2
PMDA-ODA-PEO1(20)	2.7	3.1	2.83	1.10	1.1
PMDA-ODA-PEO1(40)	5.4	27.4	1.69	16.21	5.1
PMDA-ODA-PEO1(60)	16.2	131.0	1.58	82.91	8.1
PMDA-ODA-PEO2(60)	14.2	136.3	1.72	79.24	9.6
PMDA-ODA-PEO3(60)	13.7	117.1	1.76	66.53	8.5
BTDA-ODA-PEO1(60)	10.2	80.5	1.36	59.19	7.9
6FDA-ODA-PEO1(60)	9.9	49.4	2.09	23.62	5.0
PMDA-ODA-PEO1(65)	18.4	157.0	1.57	100.00	8.5

[a] S and D in 10^{-2} $cm^3(STP)/(cm^3$ cm Hg) and 10^{-8} cm^2/s respectively.

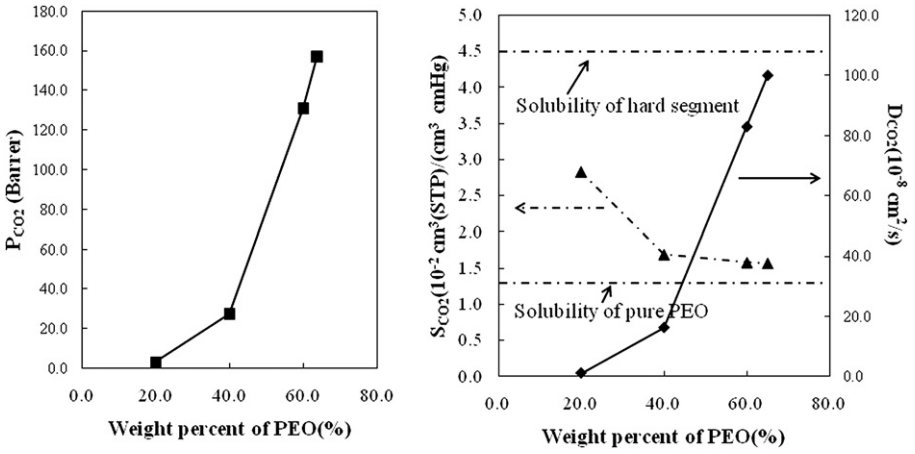

Fig. 5. Effect of PEO content on permeability, solubility and diffusivity coefficient for PMDA-ODA-PEO1.

Comparing the solubility coefficient of the pure PEO and a series of PMDA-ODA-PEO1 copolymers shown in Fig. 5, the solubility coefficients of the copolymers are well above the pure PEO line and it is very close to the solubility of pure PEO when PEO content is high. This phenomenon implies that the soft PEO phase is the main contributor to the solubility coefficient when the copolymer has high content of PEO. However, the hard segment still contributes to the total sorption even at high PEO content as the solubility of the copolymer is higher than that of pure PEO. The sorption sites in the hard segment affect the gas transport performance in the mixed gas tests which will be discussed later.

3.2.2. *Effect of PEO molecular weight*

Fig. 7 shows the permeability, diffusivity and solubility coefficient as a function of PEO molecular weight and Table 3 summarizes their corresponding CO_2/H_2 permselectivity.

At the same weight percentage of PEO in membranes, the CO_2 permeability and permselectivity increase but then decrease with an increase in PEO molecular weight. This phenomenon is a combinative result of many complicated factors. One of them is due to PEO induced crystallinity, while the other is owing to interactions between the soft and hard segments. In membranes PMDA-ODA-PEO1(60), PMDA-ODA-PEO2(60) and PMDA-ODA-PEO3(60), the degree of crystallinity increases with increasing PEO molecular weight. The crystals would act as a non-sorbing, impermeable obstacle and reduce the permeability severely. This is also reflected in the monotonous decrease in diffusivity coefficient with increasing PEO molecular weight as crystals would rigidify polymer chains and reduce the diffusivity coefficient of the resultant membrane.

The CO_2 solubility coefficient increases with increasing molecular weight of PEO used in copolymer. This could be attributed to the more complete phase separation as PEO molecular weight increases. Representative Atomic Force Microscopy (AFM) phase images, which displayed phase separation between the hard and soft segment, are shown in Fig. 8.

As can be seen from Fig. 8, the nano-sized hard phase is embedded into the PEO soft segment. The phase separation is rather not obvious in PMDA-ODA-PEO1(60). As PEO molecular weight increases, the hard phase forms fiber like nano-structured domain (Fig. 8(b)), where the two phases has much more clearer borders between them. The phase separation is even more pronounced in PMDA-ODA-PEO3(60), the separation between the two phases can be seen clearly and both phases form a bigger domain. The complete phase separation increases the interaction between the EO units and CO_2 hence the solubility coefficient is increased. Similar interactions between the soft and hard segments and their effects on micro-phase separation and permeability have been studied by Yoshino et al. [19]. They reported that the contamination (i.e., inter-penetration) of hard segments in the soft domain and soft segments in the hard domain were negligibly small if copolymers contain high molecular weight PEO. The less

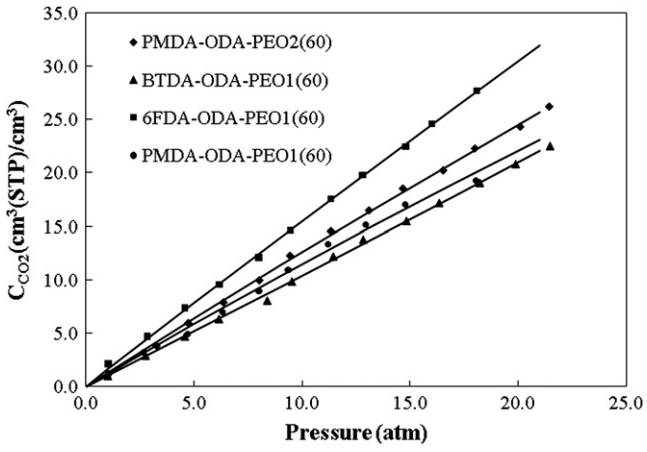

Fig. 6. CO_2 sorption isotherms in PEO block copolyimides.

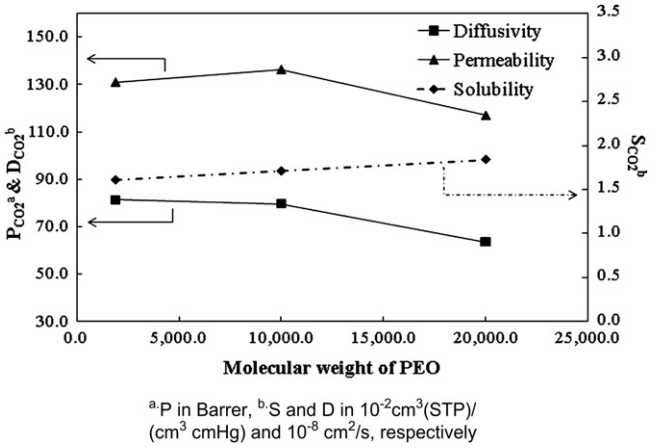

Fig. 7. Effect of PEO molecular weight on CO_2 permeability, diffusivity and solubility coefficient.

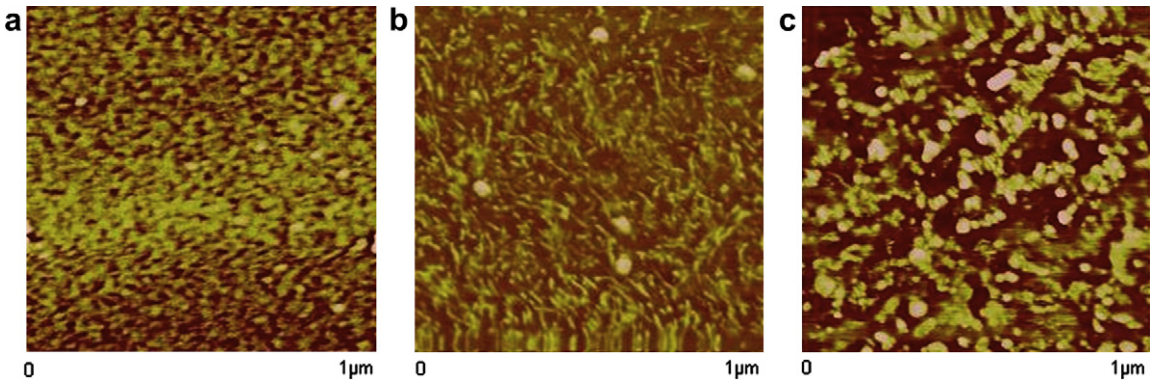

Fig. 8. AFM phase images of membrane surfaces: (a). PMDA-ODA-PEO1(60), (b). PMDA-ODA-PEO2(60) and (c). PMDA-ODA-PEO3(60).

phase inter-penetration indicates more perfect phase separation between soft and hard domains in the copolymer. As a result, copolymers containing high molecular weight PEO may facilitate the preferentially transport of penetrants through the soft segments. Since the soft segments have much higher permeability than the hard segments, the overall membrane permeability is enhanced. Another report was also published by Okamoto et al. who observed a higher CO_2 permeability for PEO containing copolyimides synthesized from a higher molecular weight PEO up to 9000 g/mol [18], this implies that the CO_2 permeability increases with increasing PEO molecular weight because of less inter-penetration or interaction between the soft and hard domains. Because the PEO induced crystallization and micro-phase separation strongly depend on PEO molecular weight and they have opposite effects on permeability, there exists an optimum PEO molecular weight in these PEO containing copolyimides in order to obtain the highest permeability and permselectivity. In this study, PMDA-ODA-PEO2(60) with a molecular weight of 10 000 g/mol possesses the highest CO_2 permeability and CO_2/H_2 selectivity which is 136.3 Barrers and 9.6, respectively.

3.2.3. *PEO percentage vs. PEO molecular weight*

When comparing the gas separation performance of the two series of PMDA-ODA-PEO copolymers as shown in Table 3; namely, one series with different PEO content and other series with different PEO molecular weights, one can conclude that the PEO content in the copolymer has stronger influence on CO_2 permeability and CO_2/H_2 selectivity than the PEO molecular weight. This phenomenon can be exemplified by the PMDA-ODA-PEO1 block copolymer where its CO_2 permeability increases from 27.4 Barrers to 131.0 Barrers when PEO content increases from 40% to 60%, while CO_2 permeability only increases from 131.0 Barrers to 136.3 Barrers when PEO molecular weight increases from 2000 g/mol to 10 000 g/mol for the copolymer containing 60% PEO. However, there is an upper limit of PEO content, as the membrane cannot be formed when the PEO content is too high. In addition, CO_2 permeability becomes very low for pure PEO membranes [39] due to high crystallinity. Furthermore, comparing separation performance of membranes synthesized from the same PEO percentage but from different PEO molecular weights, PEO-PI made from a high PEO molecular weight has a better CO_2/H_2 selectivity than that made from a low PEO molecular weight. Hence, the optimal combination of PEO content and molecular weight is the key to fabricate high performance PEO-PI membranes for gas separation.

3.2.4. *Effect of fractional free volume*

The gas separation performance of PEO-PI membranes is severely affected by the dianhydride moiety. Comparing among PMDA-ODA-PEO1(60), BTDA-ODA-PEO1(60) and 6FDA-ODA-PEO1(60), it is a surprise to notice that PMDA-ODA-PEO1(60) has the highest CO_2 permeability and CO_2/H_2 selectivity. The high CO_2 permeability is most likely attributed to the high diffusion coefficient with the aid of unique combination of chain linearity and minimal inter-penetration between the soft and rigid segments. Table 4 shows a fractional free volume (FFV) of pure polyimide. The FFV was calculated using the following equation [40]:

$$\mathrm{FFV} = (V - V_0)/V \tag{11}$$

where the specific volume, V, is calculated from the measured density; the occupied volume, V_0, is calculated from the correlation, $V_0 = 1.3V_W$, where the V_W is the van der Waals volume [41]. As for the copolymers, V_W is predicted by the equation: $V_W = m_1 \cdot V_{W1} + m_2 \cdot V_{W2}$, where m_1 and m_2 are the molar fractions and V_{W1} and V_{W2} are the van der Waals volumes of homo-polymers 1 and 2, respectively.

Since the gas diffusion rate in the soft segment is much higher than that in the hard segment. The smaller FFV value in the hard segment hinders the intrusion of PEO into the hard segment and increases the effective volume of the PEO phase which gas can penetrate through easier. In other words, the inter-penetration between the two phases will be minimized. Fig. 9 shows the AFM phase images of these three PEO-PI membrane surfaces, which gives a visual confirmation of the inter-penetration phenomenon.

Fig. 9(C) shows the two phases clearly, whereas, in 6FDA-ODA-PEO1(60), the phase separation is not obvious. This could be attributed that the higher degree of inter-penetration between the soft and hard phases. The glass transition temperatures of PEO in different dianhydride based copolymers also support our hypothesis. As can be seen in Fig. 3, all *Tg* detected in copolymers are higher than the *Tg* of pure PEO [39], this indicates different degree of contamination in the membranes. *Tg* of the three different dianhydride based copolymers follow the sequence of 6FDA-ODA-PEO1(60) > BTDA-ODA-PEO1(60) > PMDA-ODA-PEO1(60). This implies that the inter-penetration in 6FDA-ODA-PEO1(60) is the most severe one and the PEO domain in the membrane is very small, hence there is no endothermic peak corresponding to PEO melting, is observed in the DSC curve.

Table 4
FFV of pure polyimides.

Polyimide	PMDA-ODA	BTDA-ODA	6FDA-ODA
FFV	0.129	0.124	0.165

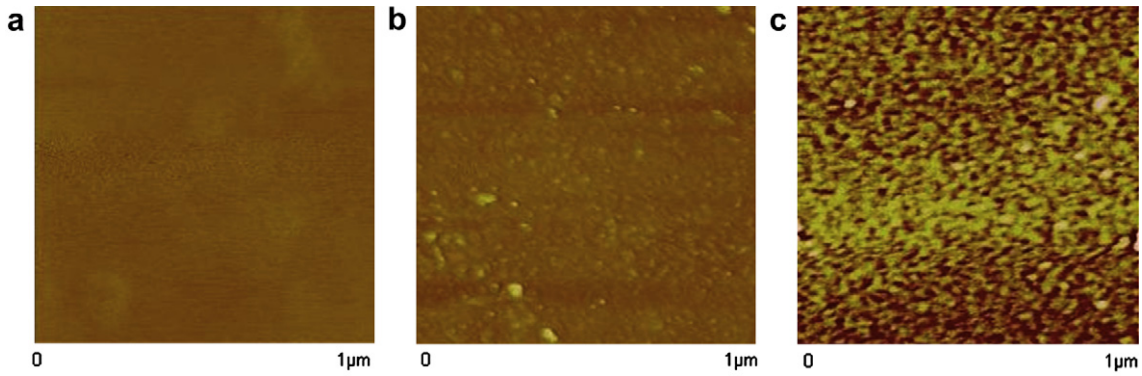

Fig. 9. AFM phase image of membrane surface: (a). 6FDA-ODA-PEO1(60), (b). BTDA-ODA-PEO1(60) and (c). PMDA-ODA-PEO1(60).

3.2.5. Mixed gas permeation tests

3.2.5.1. Improved CO_2/H_2 selectivity compared with pure gas test. Mixed gas tests were performed with a binary gas mixture of 50/50% CO_2/H_2 feeding, in which the testing temperature was 35 °C and the partial pressure of CO_2 was varied from 2 atm, 6 atm and 10 atm, respectively. Fig. 10 shows the comparison of gas transport performance between pure gas and mixed gas tests.

As can be seen from Fig. 10(A), the CO_2/H_2 selectivity in the mixed gas tests is much higher than that in pure gas tests. The drastic increment in CO_2/H_2 selectivity is mainly ascribed to the substantial decrease of H_2 permeability in the mixed gas tests as illustrated in Fig. 10(B). As the copolymer consists of hard polyimide segment and soft PEO segment, the decreased H_2 permeability can be ascribed to two factors: (1), competition of the sorption site in the hard segment; (2), weaker interaction between H_2 and polyether unit in the soft PEO phase. As mentioned in the Section 3.2.1, the hard segment in the copolymer is still permeable and contributing to the solubility coefficient even in the membranes with high PEO content. In the presence of binary gas feed stream, gas with higher condensability (CO_2) is easier to be condensed and absorbed in the membrane. As a result, the less condensable spice (H_2) would be excluded from this sorption site, which leads to the diminution of its permeability. This observation is consistent with the work done by Chern et al. [42,43]. They observed that the CO_2 permeability decreases in the presence of water molecules in the feed stream since water molecule has higher condensability and CO_2 molecules are progressively excluded from the sorption site in glassy polymeric membranes as the relative water humidity increases in the feed. Another possibility for the reduced H_2 permeability in mixed gas tests is due to the fact that H_2 has a lower interaction with ether oxygen unit in the soft PEO phase compared with CO_2. In the presence of CO_2 and H_2 gas mixture in the feed, the favorable interaction between CO_2 and ether oxygen unit hinders the permeability of H_2. The higher degree of interaction between CO_2 and the polymer matrix leads to the higher magnitude of H_2 permeability reduction. Therefore, membranes with higher content of PEO tend to have a bigger margin of H_2 reduction from pure gas tests to mixed gas tests. Fig. 10(B) shows the biggest H_2 permeability drop in PMDA-ODA-PEO1(65) which has the highest PEO content. As a result, the CO_2/H_2 selectivity shows an attractive result in the mixed gas tests.

3.2.5.2. Effect of CO_2 partial pressure in the mixed gas tests. The pressure-dependent mixed gas tests were performed at CO_2 partial pressures of 2 atm, 6 atm and 10 atm to investigate the gas separation performance of the membranes. Fig. 11 demonstrates the effect of CO_2 partial pressure on gas transport performance.

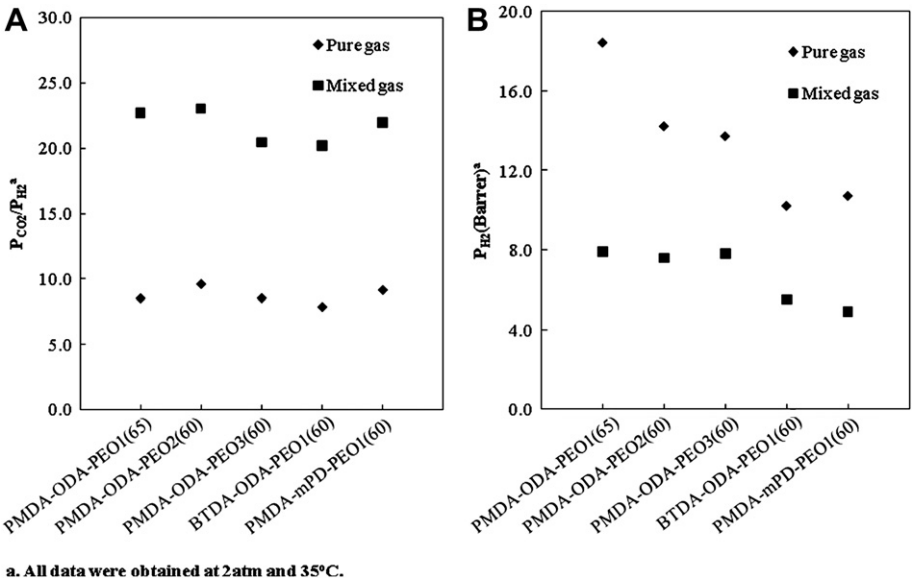

Fig. 10. Comparison of gas transport performance between pure gas and mixed gas tests.

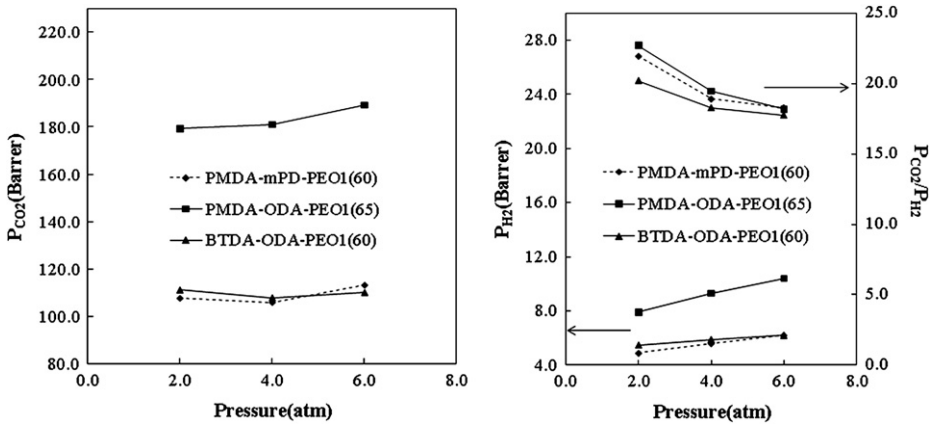

Fig. 11. Effect of CO_2 partial pressure on P_{H_2} and P_{CO_2}/P_{H_2}.

As can be seen, the H_2 permeability increases gradually and CO_2 permeability maintains or increases slightly as partial pressure of CO_2 increases. This phenomenon can be attributed to the fact that CO_2 induces chain swelling and creates the bulk flow effect as a result of increasing CO_2 partial pressure. This low magnitude of chain swelling causes greater permeability increment for smaller molecules than bigger molecules. Therefore, the gas pair selectivity decreases as the CO_2 partial pressure increases. This observation shows a good agreement with the work done by Car et al. [23], in which the CO_2 permeability in Pebax/PEG blend membranes increases slightly or stays almost the same in mixed gas tests and the CO_2/H_2 selectivity decreases as the magnitude of H_2 permeability increment is higher than CO_2.

Fig. 12 compares the mixed gas results with the upper bound of conventional membrane materials for CO_2/H_2 separation. The reverse selective membranes have a CO_2/H_2 separation performance well above the upper bound line. PMDA-ODA-PEO1 with 65% PEO content shows the best performance of CO_2 permeability and CO_2/H_2 selectivity of 179.3 Barrers and 22.7, respectively, at 35 °C and CO_2 partial pressure of 2 atm. This performance is especially impressive and valuable because the test temperature is 35 °C, not below 0 °C. Results taken from other researches for comparison purpose [22,25,26,28].

3.3. Permeability prediction by the Maxwell equation

Since PEO containing copolyimides consist of hard polyimide phases and soft PEO phases, the permeability of PMDA-ODA-PEO1 with different PEO percentages may be predicted by the Maxwell equation as shown below [44]:

$$P_{eff} = P_C\left[\frac{P_D + 2P_C - 2\phi_D(P_C - P_D)}{P_D + 2P_C + \phi_D(P_C - P_D)}\right]$$

where P_{eff} is the effective permeability, P_C and P_D are the permeability of the continuous phase and dispersed phase, respectively, and ϕ_D is the volume fraction of the dispersed phase in the block copolymer. Below are the assumptions we made in the construction of the Maxwell prediction curve, the hard polyimide phase is the continuous phase when the PEO content is lower than 40%, while the soft PEO phase is the continuous phase if the PEO content is more than 60%. In other words, there is a matrix phase transition when the PEO content is between 40% and 60%, an average value will be used as the predicted value during this transition. The permeability of pure PEO in the amorphous state (143 Barrers) is used as the permeability of the soft segments [39] since PMDA-PEO1 is unable to be synthesized in the laboratory. A permeability of 1.14 Barrers is used for PMDA-ODA as the permeability of the hard segments [45]. Fig. 13 shows the Maxwell predicted values and experimental data and a good agreement can be observed. Since the original Maxwell equation was derived to predict the resistance in a conducting medium, the predicted value is accurate only when the materials in the medium are independent to each other [44]. Therefore, the deviation observed in Fig. 13 may arise from the dependence of soft segments and hard segments in the copolymer.

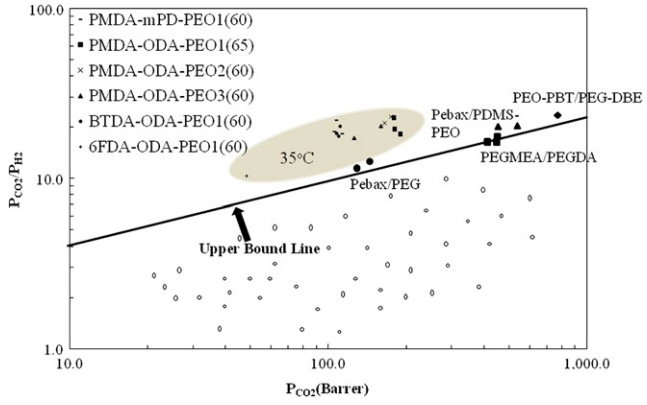

Fig. 12. Mixed gas permeation test results compared with the upper bound line.

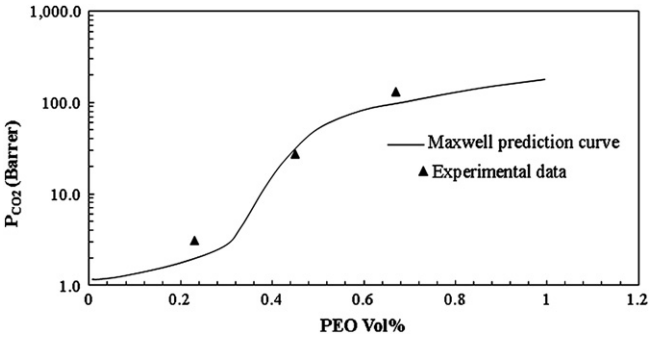

Fig. 13. Comparison between the Maxwell predicted values and experimental data.

4. Conclusion

The following conclusions can be made from this study:

1) The mechanical strength of membrane is significantly affected by the content of PEO in copolymer. It decreases with an increase in PEO content, especially when the PEO content is more than 40%, where the soft segment is forming a continuous phase.
2) In pure gas tests, the increase in CO_2 permeability of PMDA-ODA-PEO1 with increasing PEO content is attributed to the increase in gas diffusivity. The CO_2 permeability and CO_2/H_2 permselectivity experience an initial increase followed by a decrease when the PEO molecular weight in PMDA-ODA-PEO increases. Therefore, there is an optimal PEO molecular weight to be used in membrane fabrication; this optimal molecular weight provides a balance between the degree of crystallinity and micro-phase separation in order to obtain the best separation performance.
3) The FFV of the pure polyimide with different dianhydride moieties leads to different degrees of inter-penetration between the hard segments and soft segments; a higher degree of inter-penetration leads to a lower CO_2 permeability and CO_2/H_2 selectivity.
4) In mixed gas permeation tests, CO_2 permeability of 179.3 Barrer and CO_2/H_2 selectivity of 22.7 is reported for PMDA-ODA-PEO1 (65) at 35 °C and CO_2 partial pressure of 2 atm. The selectivity is much higher than pure gas tests due to CO_2 out compete H_2 for the sorption site in the hard segment and better interactions between CO_2 and the polymer matrix, which results in the reduction of H_2 permeability.

Acknowledgment

The authors would like to thank the Singapore National Research Foundation (NRF) for the support on the Competitive Research Programme for the project entitled “Molecular Engineering of Membrane Materials: Research and Technology for Energy Development of Hydrogen, Natural Gas and Syngas” with the grant number of R-279-000-261-281. The authors also thank Ms. Low BT, Mr. Lau CH, Dr. Liu SL and Dr. Li Y for giving suggestions and assistance to this work.

References

[1] Sa S, Silva H, Sousa JM, Mendes A. J Membr Sci 2009;339:160–70.
[2] Shao L, Low BT, Chung TS, Greenberg AR. J Membr Sci 2009;327:18–31.
[3] Nenoff TM, Spontak RJ, Aberg CM. MRS Bull 2006;31:735–41.
[4] Gallo M, Nenoff TM, Mitchell MC. Fluid Phase Equilib 2006;247:135–42.
[5] Yang SI, Choi DY, Jang SC, Kim SH, Choi DK. Adsorption 2008;14:583–90.
[6] Hinchliffe AB, Porter KE. Chem Eng Res Des 2000;78:255–68.
[7] Scott K. Handbook of industrial membranes. Oxford: Elsevier Advanced Technology; 1995.
[8] Perry JD, Nagai K, Koros WJ. MRS Bull 2006;31:745–9.
[9] Dai Y, Guiver MD, Robertson GP, Kang YS. Macromolecules 2005;38:9670–8.
[10] Guiver MD, Robertson GP, Dai Y, Bilodeau F, Kang YS, Lee KJ, et al. J Polym Sci Part A Polym Chem 2002;40:4193–204.
[11] Ayala D, Lozano AE, Abajo JD, Garcia-Perez C, Campa JG, Peinemann KV, et al. J Membr Sci 2003;215:61–73.
[12] Robeson LM. J Membr Sci 2008;320:390–400.
[13] Shao L, Liu L, Cheng SX, Huang YD, Ma J. J Membr Sci 2008;312:174–85.
[14] Low BT, Xiao Y, Chung TS, Liu Y. Macromolecules 2008;41:1297–309.
[15] Xiao Y, Chung TS, Chng ML. Langmuir 2004;20:8230–8.
[16] Chung TS, Shao L, Tin PS. Macromol Rapid Commun 2006;27:998–1002.
[17] Kawakami M, Iwanaga H, Hara Y, Iwamoto M, Kagawa S. J Appl Polym Sci 1982;27:2387–93.
[18] Okamoto K, Fujii M, Okamyo S, Suzuki H, Tanaka K, Kita H. Macromolecules 1995;28:6950–6.
[19] Yoshino M, Ito K, Kita H, Okamoto K. J Polym Sci Part B Polym Phys 2000;38:1707–15.
[20] Suzuki H, Tanaka K, Kita H, Okamoto K, Hoshino H, Yoshinaga T, et al. J Membr Sci 1998;146:31–7.
[21] Lin H, Freeman BD. J Mol Struct 2005;739:57–74.
[22] Car A, Stropnik C, Yave W, Peinemann KV. J Membr Sci 2008;307:88–95.
[23] Car A, Stropnik C, Yave W, Peinemann KV. Sep Purif Technol 2008;62:110–7.
[24] Husken D, Visser T, Wessling M, Gaymans RJ. J Membr Sci 2010;346:194–201.
[25] Reijerkerk SR, Knoef MH, Nijmeijer K, Wessling M. Membr Sci 2010;352:126–35.
[26] Yave W, Car A, Funari SS, Nunes SP, Peinemann KV. Macromolecules 2010;43:326–33.
[27] Zhao HY, Cao YM, Ding XL, Zhou MQ, Liu JH, Yuan Q. J Membr Sci 2008;320:179–84.
[28] Lin H, Wagner EV, Freeman BD, Toy LG, Gupta GP. Science 2006;311:639–42.
[29] Shao L, Chung TS. Int J Hydrogen Energy 2009;34:6492–504.
[30] Brandrup J, Immergut EH, Grulke EA. Polymer handbook. 4th ed. New York: John Wiley & Sons Inc; 1999.
[31] Lin WH, Vora RH, Chung TS. J Polym Sci Part B Polym Phys 2000;38:2703–13.
[32] Freeman BD, Pinnau I. Polymer membranes for gas and vapor separation, vol. 733. Washington, DC: ACS Symposium Series; 1999. pp. 1–27.
[33] Xiao Y, Shao L, Chung TS, Schiraldi DA. Ind Eng Chem Res 2005;44:3059–67.
[34] Shao L, Chung TS, Goh SH, Pramoda KP. J Membr Sci 2005;256:46–56.
[35] Wang R, Liu SL, Liu TT, Chung TS. Chem Eng Sci 2002;57:967–76.
[36] Maya EM, Munoz DM, Lozano AE, Abajo JD, Campa JG. J Polym Sci Part A Polym Chem 2008;46:8170–8.
[37] Hong S, Yang L, Macknight WJ, Gido SP. Macromolecules 2001;34:7009–16.
[38] Tanaka K, Kita H, Okano M, Okamoto K. Polymer 1992;33:585–92.
[39] Lin H, Freeman BD. J Membr Sci 2004;239:105–17.
[40] Park JY, Paul DR. J Membr Sci 1997;125:23–39.
[41] Bondi AJ. Chem Phys 1964;68:441–51.
[42] Chern RT, Koros WJ, Sanders ES, Yui R. J Membr Sci 1983;15:157–69.
[43] Chern RT, Koros WJ, Hopfenberg HB, Stannett VT. J Polym Sci Part B Polym Phys 1983;21:753–63.
[44] Maxwell JC. A treatise on electricity and magnetism, vol. 1. New York: Dover Publications Inc; 1954.
[45] Mi Y, Hirose T. J Polym Res 1996;3:11–9.